

Supplementary Information

Molecular Mechanism of 15-Lipoxygenase Allosteric Activation and Inhibition

*Hu Meng¹, Ziwei Dai², Weilin Zhang², Ying Liu^{1, 2}, Luhua Lai^{*1, 2, 3}*

¹BNLMS, State Key Laboratory for Structural Chemistry of Unstable and Stable Species,
College of Chemistry and Molecular Engineering, ²Center for Quantitative Biology,

³Peking–Tsinghua Center for Life Sciences, Peking University, Beijing 100871, China

* To whom correspondence should be addressed

Telephone: (+86)10-62757486 Fax: (+86)10-62751725 E-mail: lh lai@pku.edu.cn

Table S1. Kinetic parameters given by fitting substrate inhibition curve of 15-LOX

| Parameters | Optimal value given by fitting and 95% Credible intervals (min, max) | |
|---|--|--|
| | Activator | Inhibitor |
| K_m (mM) | 0.414 (0.939×10^{-1} , 0.503) | |
| K_m^A (mM) | 0.141 (0.261×10^{-1} , 1.72) | 0.415 (0.309×10^{-1} , 2.03) |
| K_m^S (mM) | 7.82×10^{-11} (9.40×10^{-12} , 2.70×10^{-9}) | |
| K_m^{comb} (mM) | 0.909×10^{-1} (0.134×10^{-1} , 1.01) | 4.14×10^{-11} (9.39×10^{-12} , 2.16×10^{-9}) |
| k_{cat} (s^{-1}) | 1.00×10^3 (9.33×10^1 , 1.00×10^3) | |
| k_{cat}^A (s^{-1}) | 1.26×10^2 (8.24×10^1 , 3.01×10^2) | 3.04×10^1 (8.30, 7.33×10^1) |
| k_{cat}^S (s^{-1}) | 5.48×10^{-7} (2.58×10^{-9} , 6.85×10^{-7}) | |
| $k_{\text{cat}}^{\text{comb}}$ (s^{-1}) | 3.95 (1.54, 4.97×10^1) | 6.75×10^{-8} (1.38×10^{-9} , 5.31×10^{-7}) |
| K_D^A (mM) | 2.20×10^{-3} (1.33×10^{-3} , 4.44×10^{-3}) | 8.82×10^{-5} (2.10×10^{-5} , 1.02×10^{-4}) |
| K_D^S (mM) | 7.47×10^{-4} (3.68×10^{-4} , 1.51×10^{-2}) | 8.84×10^{-5} (6.90×10^{-5} , 4.10×10^{-4}) |
| K_D^{comb} (mM) | 5.02 (5.02, 11.9) | |
| K_D^S (mM) | 9.48×10^{-10} | |

| | $(7.51 \times 10^{-10}, 6.39 \times 10^{-8})$ | |
|----------------------------|---|--|
| K_D^{Scomb} (mM) | 8.92×10^2 ($3.18 \times 10^1, 4.63 \times 10^3$) | 1.74×10^4 ($1.47 \times 10^4, 9.01 \times 10^6$) |
| K'_D^{Scomb} (mM) | 5.77×10^2 ($1.63 \times 10^1, 2.72 \times 10^3$) | 1.73×10^{-6} ($1.73 \times 10^{-6}, 9.57 \times 10^{-3}$) |
| K_D^{Acomb} (mM) | 1.83×10^{-6} ($2.74 \times 10^{-8}, 1.18 \times 10^{-5}$) | 3.31×10^{-8} ($9.84 \times 10^{-11}, 6.70 \times 10^{-7}$) |
| K'_D^{Acomb} (mM) | 2.1×10^3 ($3.89 \times 10^1, 4.42 \times 10^3$) | 1.75×10^{-8} ($9.83 \times 10^{-11}, 5.36 \times 10^{-7}$) |

Table S2. Comparison of the results from CAVITY and SiteMap.

| Analysed Protein Structure | Detected Binding sites | CAVITY Score ^a | Volume given by CAVITY (\AA^3) | SiteMap Score ^b | Volume given by SiteMap (\AA^3) |
|----------------------------|-----------------------------------|---------------------------|---|----------------------------|--|
| Starting conformation | Catalysis site | 10.0 | 885 | 1.12 | 365 |
| Starting conformation | Allosteric regulator binding site | 10.2 | 883 | 1.09 | 483 |
| Apo 15-LOX Cluster-1 | Catalysis site | 10.7 | 1489 | 1.04 | 924 |
| Apo 15-LOX Cluster-1 | Allosteric regulator binding site | 11.0 | 882 | 1.11 | 442 |

^aHigher score means a higher possibility this site to be a real binding site.

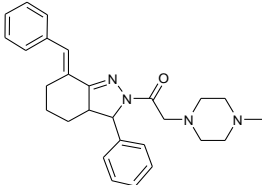
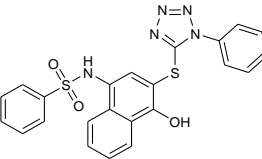
^bHigher score means a higher possibility this site to be a real binding site.

Table S3. Residues in different communities.

| Community ID Number | Apo | With Acitvator | With inhibitor |
|------------------------|---------------------------------------|--|--|
| 1 | 1-18, 41-101, 111 | 1-19, 41-103, 111-115, 615-616 | 1-19, 41-99, 163 |
| 2 | 132-154, 368-379, 437-440, 493-519 | 2 & 12: 132-153, 356-379, 425-436, 492- 518, 660 | 132-153, 356-379, 437, 483, 485-520 |
| 3 | 155-182 | 154-172, 395-312, 661-332 | 154-178, 387-409, 661 |
| 4 | 212-222, 336-349, 351, 546-557 | 212-223, 336-355, 553-557, | 4a: 202-221, 543-552, 590-603 <hr/> 4b: 222-228, 336-355, 553-559 |
| 5 | 112-131, 380-383 | 115-130 | 111-131, 380-386 |
| 6 | 211-245, 271-350, 454-459 | 224-245, 272-335,450-451 | 6 & 11: 225-335, 450, 565-569 |
| 7 | 384-402, 610-613, 615, 659, 661 | 131, 381-394, 533-542, 604-608, 648-659 | |
| 8 | 392, 472-491, 520-533, 622 | 8 & 15: 437-491, 519-532 | 8 & 15: 234, 438-484, 521-533 |

| | | | |
|----|--|------------------------------|---------------------------------------|
| 9 | 541-658 | 9a: 609-647 | 534-660, 662 |
| | | 9b: 543-603 | |
| 10 | 283-296, 339, 403-423, 558-591 | 285-296, 413-424, 558-587 | 10 & 12: 282-296, 410-436, 560-589 |
| 11 | 246-270 | 246-271 | |
| 12 | 352-367, 424-436, 534-540, 660, 662 | | |
| 13 | 19-40, 57-110 | 20-40, 57-110 | 20-40, 57-110 |
| 14 | 183-211 | 173-211 | 179-202 |
| 15 | 439-471 | | |

Table S3. Activity of PKUMDL_MH_1001-2 in the Cell-free Assay. ^a

| Compound | SPECS ID | Structure | EC ₅₀ (μ M) | Max Activation or Inhibition | K _D determined by SPR (μ M) |
|----------------------------|---------------------|---|--------------------------------|------------------------------------|--|
| PKUMDL_ MH_1001 | AO-476/4 3305824 |  | 6.8 \pm 0.4 | 85% Activation | 3.9 \pm 0.1 |
| PKUMDL_ MH_1002 | AQ-390/4 3238223 |  | 0.7 \pm 0.1 | 100% Inhibition | 1.7 \pm 0.1 |

^a Data shown represent the mean \pm SEM (n = 3);

Table S4. EC₅₀ of PKUMDL_MH_1001 and PKUMDL_MH_1002 to 15-LOX mutants in Cell-free Assay. ^a

| Enzyme | Initial reaction rate without any compound ($\mu\text{M s}^{-1}$) | EC ₅₀ (μM) and maximum activation or inhibition (%) | |
|--------------|---|---|----------------------------|
| | | PKUMDL_MH_1001 (Activator) | PKUMDL_MH_1002 (Inhibitor) |
| Wild Type | 0.175 \pm 0.003 | 6.8 \pm 0.4 (85%) | 0.7 \pm 0.1 (100%) |
| R242A | 0.023 \pm 0.001 | 51 \pm 7 (400%) | 4.7 \pm 0.9 (100%) |
| E275A | 0.062 \pm 0.005 | 8.6 \pm 1.0 (272%) | 2.6 \pm 1.0 (100%) |
| D277A | 0.154 \pm 0.005 | n.d. ^c (0%) | 1.0 \pm 0.4 (100%) |
| F435A, S440A | 0.083 \pm 0.007 | 3.6 \pm 0.8 (251%) | 3.4 \pm 1.4 (100%) |

^a Data shown represent the mean \pm SEM (n = 3); ^b Enzyme concentration is 10 $\mu\text{g/mL}$; ^c n.d., not determined due to weak activation. Data shown represent the mean \pm SEM (n = 3).

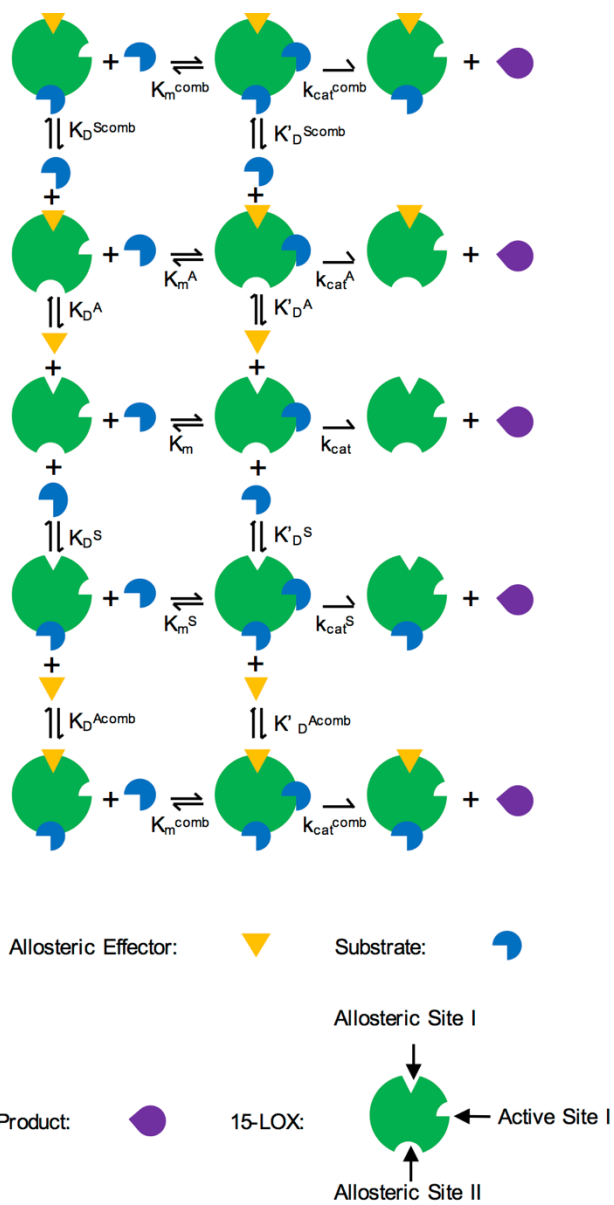


Figure S1. Scheme of substrate inhibition mechanism.

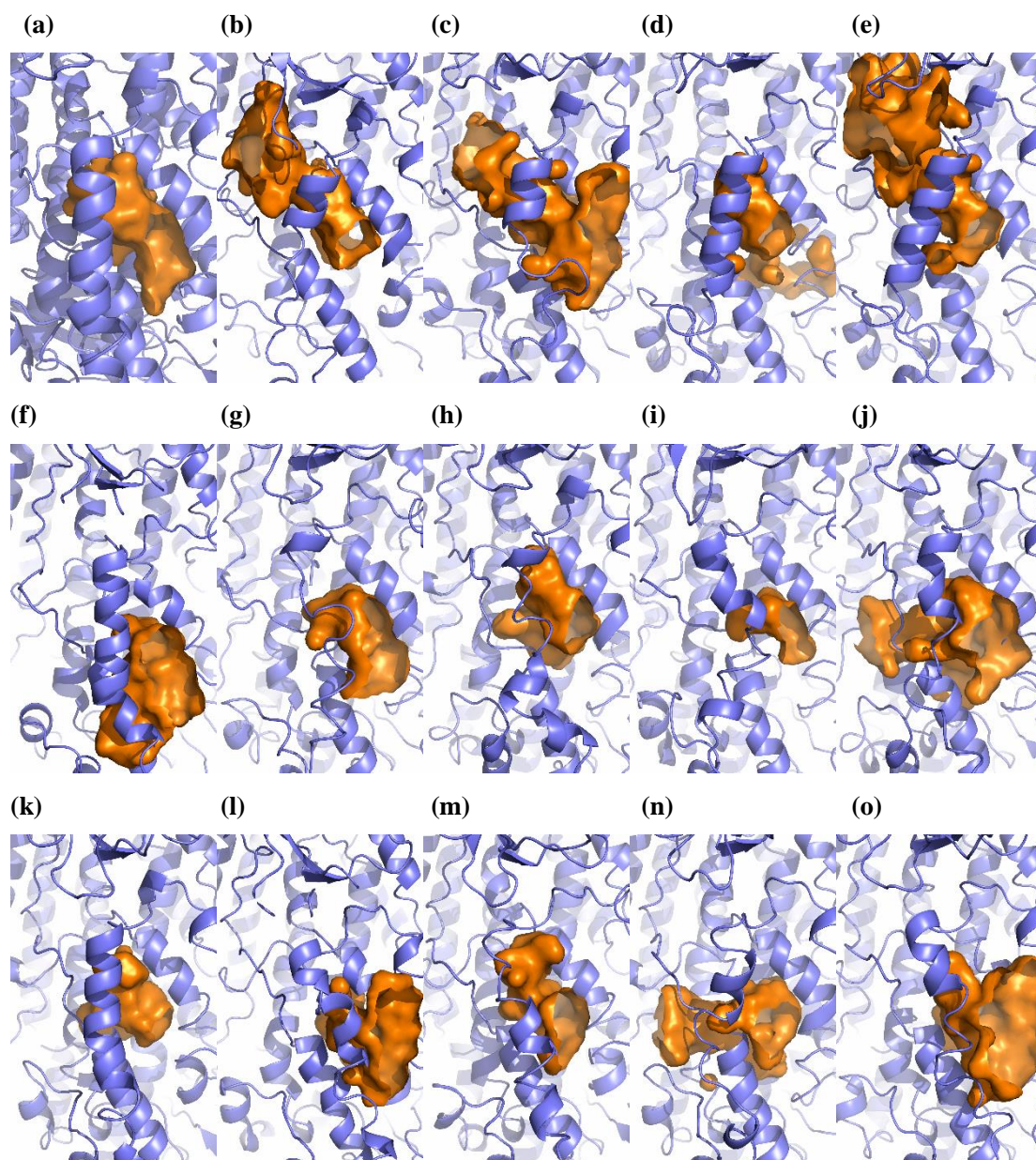
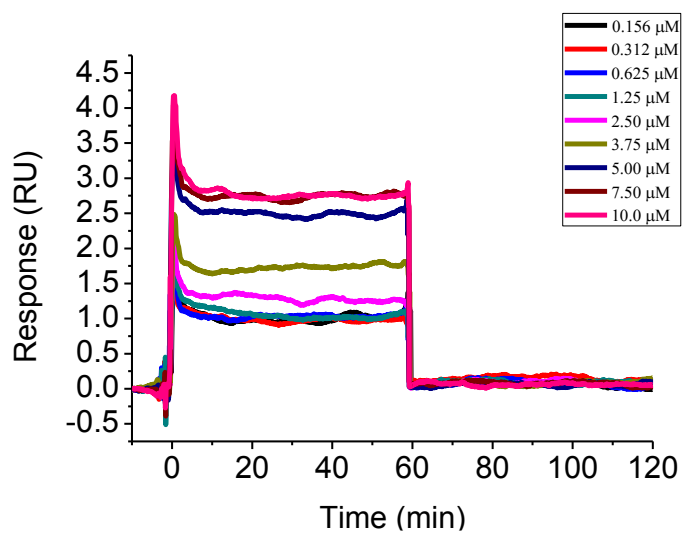


Figure S2. The surfaces of cavities at active site in the representative conformations of apo 15-LOX, 15-LOX with activator, and 15-LOX with inhibitor in the last 10-ns of MD simulations

The surfaces of cavities at active site in the representative conformations of (a) starting conformation, (b)-(e) apo 15-LOX, (f)-(j) 15-LOX with activator, and (k)-(o) 15-LOX with inhibitor in the last 10-ns of MD simulations were also shown in this figure. (b) to (o) are middle conformations of cluster 1 to 14, respectively.

a. PKUMDL_MH_1001:



b. PKUMDL_MH_1002:

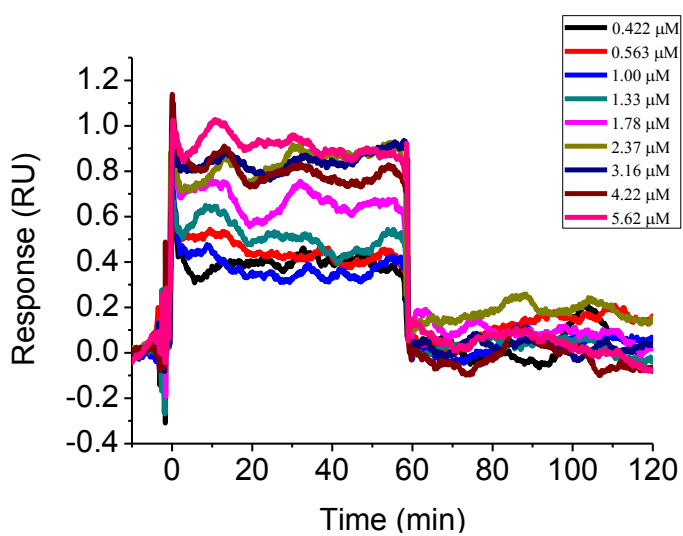


Figure S3. Surface Plasmon Resonance data of PKUMDL_MH_1001-2 binding with immobilized 15-LOX.

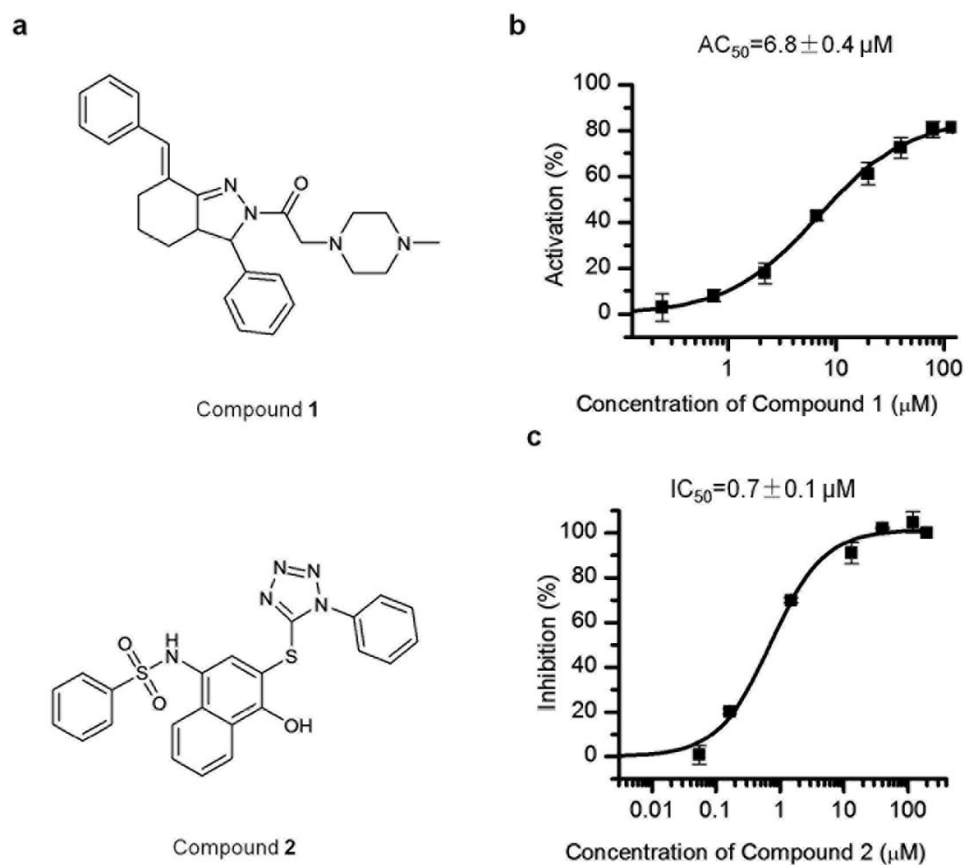


Figure S4. Structures and dose–response curves of compounds 1-2 in cell free assay.

(a) Molecular structures of compounds 1-2; (b) dose-response curves of compound 1, (c) compound 2.

Supplementary Methods

Quantum mechanics

We sought parameters for pseudobonds to the Fe^{2+} center to maintain the geometry of this coordinated metal center during the fast timescales of the simulation. We started

with a model system consisting of Fe::methyl-imidazole or Fe::methyl-carboxylate. We performed geometry optimization in Jaguar (Schrodinger, Inc.) using DFT(B3LYP) with basis set 3-21G*. We identified the lowest frequency involving the Fe-N or Fe-O stretch using a visualization of frequencies in Maestro (Schrodinger, Inc.) in order to obtain an approximate bond force constant of 103.425 kcal/mol/Å² for His N-Fe and 274.71 kcal/mol for O-Fe. Angle restraints were automatically generated during Desmond system preparation with a force constant of 60 kcal/mol/rad². The equilibrium distances for these bonds were set equal to those in the initial geometry for minimal perturbation in the crystal structure. Although this technique provides only an approximate force constant, the presence of five bonds to the iron center, the centrality of the site in the core of the protein, and the short timescales of the simulations (tens of ns) support the appropriateness of this approach for the purposes of the present work, which does not require detailed catalytic mechanism at the active site.

Molecular dynamics simulations

We performed Molecular dynamics simulations in explicit solvent with the Desmond¹ software package with the OPLS-AA/SPC force field². The protein was placed in an orthorhombic simulation with a buffer of 10Å on each side. Na⁺ and Cl⁻ ions were added to neutralize the system, and then 0.05 M NaCl was added. Minimization was first performed with the solute positions restrained at 50 kcal/mol/Å for 2000 steps or convergence of 50 kcal/mol/Å² with 10 steepest-descent steps. The solute positions

were unrestrained, and minimization proceeded for another 2000 steps or until a convergence of 50 kcal/mol/Å² was achieved.

Next, solute heavy atoms were restrained at 50 kcal/mol/Å. NVT molecular dynamics were performed at 10 K for 12 ps with 1 fs time steps for the bonded and short-range non-bonded interactions and 3 fs time steps for the long-range interactions. The Berendsen thermostat was used with a relaxation time of 0.1 ps⁻¹ and a re-sampling period of 1 ps. This was followed by NPT equilibration at 10 K for 12 ps using 1 fs time steps for the bonded and short-range non-bonded interactions and 3 fs time steps for the long-range interactions with the Berendsen thermostat and barostat. The thermostat relaxation rate was set to 0.1 ps⁻¹, and the barostat relaxation rate was set to 50 ps⁻¹ with a re-sampling period of 1 ps. Next, the time step was increased to 2 fs for the bonded and short-range non-bonded interactions, and long-range non-bonded interactions were updated every 6 fs. NPT equilibration was performed at 10 K for 12 ps with the Berendsen thermostat and barostat using a thermostat relaxation rate of 0.1 ps⁻¹, a barostat relaxation rate of 50 ps⁻¹, and a re-sampling period of 1 ps. Then, the system was simulated for another 34 ps at 300 K using the same settings. Finally, heavy atom position restraints were removed, and the system was simulated for an additional 24 ps at 300 K with a thermostat relaxation rate of 0.1 ps⁻¹ and barostat relaxation rate of 2 ps⁻¹.

After minimization and equilibration, multiple (different random seed) production runs of 10 ns were performed on each system using the Martyna-Tobias-Klein integrator³ at 300 K and 1 atm. Snapshots were taken every 1.0 ps. All bonds with

hydrogens were constrained. A 2 fs time step for the bonded and short-range non-bonded interactions was used. Long-range non-bonded interactions were updated every 6 fs using the RESPA multiple time-step approach. Short-range coulombic and van der Waals non-bonded interactions were cut off at 9.0 Å, and long-range electrostatics were computed using the smooth particle-mesh Ewald method. Pair lists were constructed using a distance of 10.5 Å and a migration interval of 12 ps. Production runs were collected as follows. In total, 104 ns of production molecular dynamics were collected for each system.

Molecular Cloning, Protein Expression, and Purification of 15-LOX.

Wild-type human *15-LOX* was amplified into the pET-28 system from a cDNA (MGC:34638 IMAGE:5179700) clone purchased from Source BioScience with the primers LOX-Nde-F (5'-TGTACATATGGGTCTCTACCGCATCCGCGTGTC-3') and LOX-Xho-R (5'-ACGACTCGAGTTAGATGGCCACACTGTTTTCCACC-3'). The PCR product and the vector pET-28a were digested with NdeI and XhoI. The amplified fragments of *15-LOX* were ligated into the pET-28a vector with T4 DNA ligase. The residue P461 in the original cDNA did not agree with the corresponding residue in the human genome, which was A461. We mutated the proline to alanine using the QuikChange site-directed mutagenesis kit. The resulting plasmid pET-*15LOX*-h28 encoded the 15-LOX protein with an N-terminal His6 tag. Mutations were introduced into *15-LOX* with the QuikChange site-directed mutagenesis kit (Stratagene) with pET-*15LOX*-h28 as a template.

pET-*15LOX*-h28 and mutants were transformed into *E. coli* strain Rosetta <DE3> for expression of His6-tagged 15-LOX (His6-15LOX) and His6-tagged mutant proteins.

Cells were cultured at 37 °C in LB media containing Fe²⁺ (50 μM), kanamycin (34 μg mL⁻¹), and chloramphenicol (30 μg mL⁻¹). At an A600 of about 1.0, isopropyl β-D-thiogalactopyranoside was added to a final concentration of 0.5 mM. Cells were grown for an additional 12 h at 22 °C, harvested, resuspended in lysis buffer [Tris-HCl (50 mM, pH 8.0), NaCl (100 mM), 1,4-dithiothreitol (DTT 1 mM), and phenylmethylsulfonyl fluoride (1 mM)], and lysed by ultrasonic treatment.

The supernatant of the lysate was applied to a nickel-nitrilotriacetic acid column (HisTrap HP; GE Healthcare) equilibrated with buffer A [Tris-HCl (50 mM, pH 8.0), NaCl (100 mM), and imidazole (10 mM)]. The protein bound to the resin was then eluted with buffer B [Tris-HCl (50 mM, pH 8.0), NaCl (100 mM), and imidazole (200 mM)]. The eluted enzyme was desalted and applied to an anion-exchange column (Q Trap HP; GE Healthcare) equilibrated with buffer C [Tris-HCl (20 mM, pH 8.0), DTT (1 mM)]. The protein bound to the resin was then eluted with a gradient of 10–100% buffer D [Tris-HCl (20 mM, pH 8.0), DTT (1 mM), and NaCl (1 M)]. All buffers were degassed before use, and the whole purification approach was performed at 4 °C.

The purities of protein samples were confirmed by SDS/PAGE on a polyacrylamide gel (10 %, w/v) with a mini-vertical gel system (Bio-Rad). Bands were visualized by staining with Coomassie Brilliant Blue. Protein concentrations were determined by absorbance at 280 nm with an extinction coefficient of $1.20 \times 10^5 \text{ M}^{-1} \text{ cm}^{-1}$.

Surface Plasmon Resonance Experiments

The binding affinity of PKUMDL_MH_1001-2 towards 15-LOX was assayed using the SPR-based Biacore T200 instrument. 15-LOX was immobilized on a CM5 sensor chip by using standard amine-coupling at 25°C with running buffer HBS-P (20 mM phosphate buffer, 2.7 mM NaCl, 137 mM KCl, 0.05% surfactant P-20, pH 7.4) as described previously.⁴ In the direct binding experiments between 15-LOX and PKUMDL_MH_1001-6, 15-LOX immobilization level was fixed at 800 response units (RU), and then different concentrations of PKUMDL_MH_1001-6 containing 5% DMSO were serially injected into the channel to evaluate binding affinity. Regeneration was achieved by extended washing with the running buffer after each sample injection. The equilibrium dissociation constants (KD) of the PKUMDL_MH_1001-2 were obtained by fitting binding response units to Hill equation.

1. K. J. Bowers, E. Chow, H. Xu, R. O. Dror, M. P. Eastwood, B. A. Gregersen, J. L. Klepeis, I. Kolossvary, M. A. Moraes, F. D. Sacerdoti, J. K. Salmon, Y. Shan and D. E. Shaw, presented in part at the Proceedings of the ACM/IEEE Conference on Supercomputing (SC06), Tampa, Florida, November 11-17, 2006.
2. G. A. Kaminski, R. A. Friesner, J. Tirado-Rives and W. L. Jorgensen, *J. Phys. Chem. B*, 2001, **105**, 6474-6487.
3. S. Melchionna, G. Ciccotti and B. L. Holian, *J. Chem. Phys.*, 1996, **105**, 346-347.
4. Q. Wang, Y. F. Qi, N. Yin and L. H. Lai, *PLoS ONE*, 2014, **9**.